X-ray diffraction studies of the structures of dynamically compressed Be, Al, LiF, KCl, and Fe + 3%Si

L. A. Egorov, A. I. Barenboĭm, N. G. Makeev, V. V. Mokhova, and V. G. Rumyantsev
(Submitted 31 March 1992; resubmitted 7 September 1992)
Zh. Eksp. Teor. Fiz. **103**, 135–150 (January 1993)

We have recorded nonequilibrium structural states under dynamical pressures up to 23 GPa in all substances that were studied. Nonequilibrium arises in the shock front as a result of uniaxial deformation of the initial structure of the sample. For beryllium, deformation occurred along the C axis—the height of the hexagonal prism; for crystals in the cubic system deformations occur along the ⟨111⟩ axis. The diffraction patterns of potassium chloride indicate that the primary uniaxial deformation processes in the initial structure are identical and that the structure subsequently transforms into an equilibrium state at pressures below and above the phase-transformation point.

1. INTRODUCTION

A method for performing x-ray diffraction investigations of the structures of dynamically compressed materials has been under development for the last two decades.[1–3] The diffraction patterns obtained demonstrate the behavior of the structures of solids under rapid deformations.[4–6] The method is of interest because it is currently the only direct method for microscopic study of the structure of materials directly behind the shock front. The method can be employed for studying the mechanism of plastic flow of cyrstals under dynamical compression as well as for developing more accurate models for interpreting experimental Hugoniot-adiabat data.

The short lifetimes of dynamical states of the materials under study (fractions of μsec) make it difficult to study dynamically compressed polycrystals by this method. The problem is partially solved by using high-intensity x-ray pulses and efficient means for making diffraction photographs.[1,3,7–11] The solution of the problem can be facilitated by using data for single-crystal samples compressed in different cyrstallographic directions, which simplifies the problem of making diffraction photographs, because significantly more matter is located in a reflecting position in the case of a single crystal than in a polycrystal. In addition, single crystals give simpler diffraction patterns, because it is obvious that in this case effects caused by a single crystal and not the average effect from a large number of arbitrarily oriented crystallites will be observed.

We present below the results of measurements of the structural parameters of dynamically compressed polycrystalline samples of beryllium, silicon iron, and aluminum (the alloy AD-1) as well as single-crystal samples of lithium fluoride and potassium chloride. The measurements cover the pressure range 2–23 GPa. The photographs demonstrate the disequilibrium of the structural states that are realized and the uniformity of the compression of the material, which, to within the errors of measurement, is equal to the hydrostatic compression of the sample.

2. EXPERIMENTAL ARRANGEMENT

The instrumentation complex described in Ref. 1, together with the geometry of the experiments, was used in our studies. A plane shock wave, which compressed the sample, was generated with the help of a system consisting of an explosion lens and a cylindrical explosive charge 90 mm in diameter. A striker-screen was placed between the sample and the face of the explosive. The combination of the type of explosive and the type of material employed for the screen determined the pressures produced in the sample. The widths of the gaps between the explosive and the screen and between the screen and the sample were chosen so as to ensure constant pressure during the measurements. The characteristics of explosive shock-wave generators are described in greater detail in Ref. 12.

Textured samples, the predominant orientation of whose crystallites made it possible to obtain reflections from the (011) planes of the beryllium structure, the (110) plane of the silicon iron structure, and the (111) and (200) planes of the aluminum structure, sufficient for recording the intensity in the pressure range studied, were used in order to increase the reflectivity of the polycrystals.

Single-crystal lithium fluoride and potassium chloride samples with three orientations were used: ⟨110⟩, ⟨111⟩, and ⟨100⟩. The sample with ⟨hkl⟩ orientation (⟨hkl⟩ sample) was cut from a single-crystal block (the characteristic dimensions of the sample were $20\times 15\times 3$ mm^3) in a manner so that the crystallographic direction ⟨hkl⟩ was perpendicular to the 20×15 mm^2 surface studied. When the striker stopped against the studied surface, a shock wave, which compressed the sample in the crystallographic direction corresponding to its orientation, was generated. The choice of sample orientations covers the measurements of the interplanar spacings of the three most closely packed families of crystallographic planes (111), (200), and (220) of the lattice of the initial fcc structure of the samples.

Any deviation from parallelism of the plane of the shock front and crystallographic plane under study was determined, on the one hand, by the precision of the mechanical working of the samples and, on the other, by the deflection of the shock front from a plane and its inclination with respect to the axis of the explosive, and fell into the range $\pm 1°$.

The measurement procedure consisted of the following.

1. A diffraction peak from the initial state of the sample structure and a diffraction peak of a standard (reference) material are recorded on a preliminary photograph.

2. The reflection from the reference and the reflection

 1063-7761/93/010073-09$10.00

from the structure of the compressed material are recorded on a dynamical photograph. The reference was not subjected to dynamical action; this made it possible to reconstruct on the dynamical photograph the position of the diffraction peak of the initial structure.

3. Having on a dynamical photograph a peak of the initial structure with known diffraction angle, the diffraction angle of the reflection from the structure of the compressed material can be determined. The coordinate of the maximum of the optical density of the peak was taken as the coordinate of the peak.

The accuracy with which the interplanar spacing is measured is related to the accuracy with which the diffraction angle is measured.[13] The latter accuracy was determined by the spread in the values of the parameters of the recording scheme and its range was $\pm 0.05°$. This gave a relative error of measurement of the interplanar spacing of not worse than 0.5%. Subsequent estimates of the structural parameters and the quantitites derived from them are presented within this accuracy.

3. EXPERIMENTAL RESULTS AND DISCUSSION

3.1. Beryllium

Figure 1 displays a fragment of the diffraction pattern of the structure of a beryllium sample compressed by a shock wave with pressure amplitude $P = 22.8 \pm 0.4$ GPa. The bulk compression of the sample is $\sigma = D/(D-u) = 1.16 \pm 0.01$, where D is the velocity of the shock wave and u is the mass velocity of the material behind the shock front. The Hugoniot-adiabat data for beryllium, aluminum, and lithium were taken from Ref. 14. The diffraction reflections from the (010) and (011) planes of the hcp structure of beryllium are recorded in the photograph. It is sufficient to know the angular distance between the (010) and (011) peaks and the volume of the hexagonal cell in order to determine uniquely the cell parameters: $a = 2.28 \pm 0.01$ Å and $c = 3.1 \pm 0.01$ Å. The volume of the hexagonal cell was taken to be the cell volume of the initial state of the structure of the sample reduced by a factor of σ. Comparison with the parameters of the initial state of the beryllium structure—$a_0 = 2.286$ Å and $c_0 = 3.584$ Å (Ref. 15)—shows that, to within the measurement error, the cell is compressed along a single crystallographic direction (the C axis is compressed) and it does not depend on the orientation of this direction with respect to the shock front.

The experimental data characterizing the behavior of the beryllium structure in an unloading wave were obtained by stopping against the sample a 1 mm thick polyethylene striker moving with speed $W = 3$ km/sec. In this case, a constant-flow regime with pressure amplitude $P = 20$ GPa is realized in the sample; after a time $\approx 0.3\,\mu$sec this regime is replaced by a regime determined by the unloading wave arriving from the free surface of the striker and completely unloading the investigated layer of matter within an additional $\approx 0.3\,\mu$sec. The x-ray diffraction data indicate that the expansion of the beryllium structure in the wave of unloading from a state with pressure $P = 20$ GPa is uniaxial, and the expansion occurs along the C axis.

3.2. Silicon iron

The silicon iron (Fe + 3 wt.% Si) structure exhibits dynamical deformation of the same uniaxial character. It is well known that silicon iron with low silicon concentrations (up to 15%) is a substitutional solid solution and under normal conditions it has a bcc structure whose edge length depends on the silicon concentration.[16] For 3% silicon content $a_0 = 2.862$ Å. Figure 2 displays a fragment of the diffraction pattern of the structure of the silicon iron sample under pressure $P = 6.8 \pm 0.2$ GPa and $\sigma = 1.04 \pm 0.01$. The

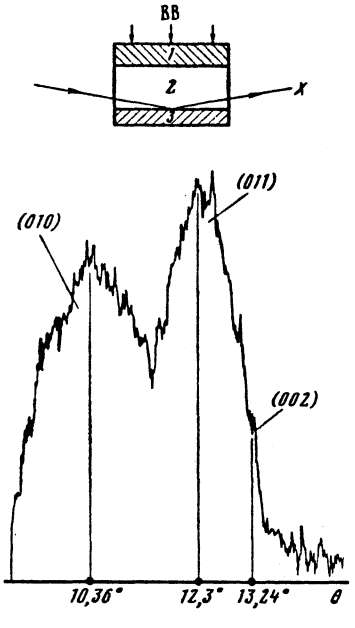

FIG. 1. Diffraction photograph of beryllium structure under pressure $P = 22.8$ GPa, $\sigma = 1.16$, and the geometry of the dynamical loading assembly: 1—striker (Al) with thickness $L = 6$ mm, velocity $W = 3.65$ km/sec; 2—Li layer ($L = 15$ mm); 3—sample; X—x-ray.

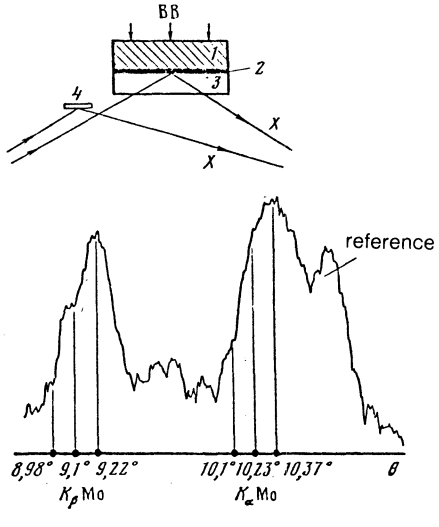

FIG. 2. Diffraction photograph of the structure of silicon iron under pressure $P = 6.8$ GPa, $\sigma = 1.04$; 1—striker (Cu, $L = 10$ mm, $W = 0.62$ km/sec); 2—sample ($L = 0.3$ mm): 3—screen (Be, $L = 5$ mm); 4—diffraction reference: RS—reference signal.

Hugoniot-adiabat data were taken from Ref. 17 for silicon iron and Ref. 14 for silicon. In estimating the volume compression of the sample, we neglected the pressure relaxation caused by the difference in the dynamical impedances of copper, silicon iron, and beryllium in the investigated layer of matter. This is permissible if the small difference between the dynamical adiabats of copper and silicon iron at pressures up to 14.6 GPa, i.e., up to the critical pressure of the phase transformation in the sample,[17] is taken into account. The photograph recorded three peaks with diffraction angles θ_i and the corresponding interplanar spacings d_i:

$\theta_1 = 10{,}1°$, $d_1 = 2{,}024$ Å;
$\theta_2 = 10{,}23°$, $d_2 = 1{,}999$ Å,
$\theta_3 = 10{,}37°$, $d_3 = 1{,}972$ Å.

The recorded result can be understood as the realization of two states: One state, determined by the angle $\theta_2 = 10.23°$, is an equilibrium state and has the bcc structure with edge length $a = a_0\sigma^{-1/3}$, i.e., an isotropically compressed cell of the initial structure. The other is a nonequilibrium state, determined by the two remaining peaks and is a distorted bcc structure with the angle between the edges different from 90° and cell volume equal to the volume of the initial cell reduced by a factor of σ. Such a deformation of a bcc structure can be obtained, if one of the body diagonals of the cubic cell is compressed by a factor of σ. Then the primitive rhombohedron, on which the bcc structure is based, and for which the angle $\alpha = 109.46°$ between the edges,[18] transforms into a rhombohedron with $\alpha = 110.16°$, and the (110) peak of the initial structure splits into two peaks, one of which ($\theta_1 = 10.1°$) is not shifted while the other is shifted into a position determined by the angle $\theta_3 = 10.37°$.

The analogy with the behavior of the beryllium structure becomes clearer by switching to a hexagonal cell in the description of the bcc structure. On switching to hexagonal basis vectors, the (110) reflection indices of the bcc structure separate into two groups: (110) and (101). The [001] direction (the C axis) of the hexagonal prism is the axis of the zone to which the (110) plane refers. On deformation along the zone axis, not all interplanar spacings in the system of planes in this zone change. The interplanar spacings of the (101) planes, which make a finite angle with the direction of deformation, decrease, and this results in splitting of the (110) peak of the bcc structure.

The diffraction photographs of the silicon iron structure at pressure $P = 9.4$ GPa, which were obtained in the dynamical loading geometry similar to that of Fig. 1, demonstrate the realization in the observed part of the material of only the nonequilibrium structural component in an orientational position with respect to the shock front, when only one dynamical peak, coinciding with the (110) peak of the initial structure, is present in the photograph. This result agrees qualitatively with the data of Ref. 19, since measurements of the diffraction angles, obtained from the silicon iron structure under analogous conditions of dynamical loading were not performed in Ref. 19.

3.3. Lithium fluoride

The characteristic feature of the diffraction photographs of lithium fluoride which are presented in Fig. 3 is the splitting of the peak of the initial structure in the dynamical photograph into two peaks. The peak with the larger diffraction angle corresponds to an equilibrium state of the compressed structure. The relation between the interplanar spacing d, determined by the peak of the equilibrium structure of the compressed material, and the interplanar spacing d_0, determined by the peak of the initial structure, is given by $d = d_0\sigma^{-1/3}$, i.e., the cell of the structure of the dynamically compressed material is equal to the isotropically compressed material with the cell volume of the initial structure decreased by a factor of σ. The peak with the smaller diffraction angle coincides with the peak recorded in the preliminary photograph. The existence of this peak in the dynamical photograph can be explained as being the result of either a reflection from the planes of the structure of the uncompressed material or a reflection from planes of the structure of the compressed material. The first case is possible: a) if the irradiation of the material starts before the shock wave arrives at the investigated surface of the sample, and b) if the irradiation occurs at later times—from a layer of the material encompassed by lateral unloading.

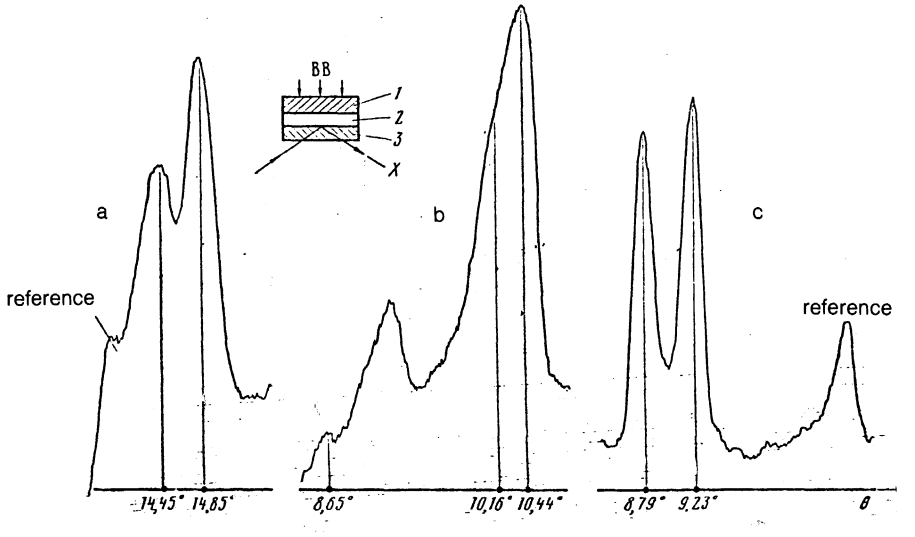

FIG. 3. Diffraction photograph of ⟨110⟩ (a), ⟨100⟩ (b), and ⟨111⟩ (c) lithium chloride structures under pressure $P = 6.6$ GPa, $\sigma = 1.08$ (a,b) and $P = 13.5$ GPa, $\sigma = 1.16$ (c): 1—striker Al, $L = 10$ mm, $W = 1.6$ km/sec); 2—sample ($L = 3$ mm); 3—layer of plexiglas (a,b) or Be (c), $L = 5$ mm. In Fig. 3b the reflection from the (110) planes of the rhombohedron with diffraction angle $\theta = 10.16°$ is superposed on the reflection from the (200) plane of the fcc structure with $\theta = 10.44°$ and is seen as a shoulder of a stronger reflection. These same reflections, formed by K_βMo anode radiation, can be seen on the left; further to the left the (100) peak of the structure of the rhombohedron can be seen.

Control experiments showed that the irradiation of the material $\approx 0.5\,\mu$sec after the arrival of the shock wave at the investigated surface does not change the diffraction pattern. In this case, the material in the layer of the sample studied and encompassed by the lateral unloading wave does not give a diffraction reflection with the same angular position as the diffraction peak of the initial structure. The latter assertion was checked by screening the investigated layer of the material, located in the constant-flow region, from the x-rays by a thin (0.05 mm thick) lead foil placed between the sample and the support layer 3 (Fig. 3a); this resulted in vanishing of both peaks in the photograph. We are left with the second proposition—both peaks were recorded from the structure of the compressed material. Hence it follows that a mixture of two structural states was recorded in the photographs: One state is identical to the isotropically compressed initial structure of the sample and the other state is a nonequilibrium state characterized by preservation of the interplanar spacing of the system of crystallographic planes of the initial structure which are oriented parallel to the shock front.

The results of x-ray diffraction investigations of dynamically compressed single crystals of lithium fluoride are presented in Refs. 20–22. The diffraction patterns were recorded by a method different from the one employed in the present work in that there was no support layer 3 (Fig. 3); a thin layer of the material under study (10–20 μm thick) played the role of the support layer. The required synchronization of the irradiation of the sample with the instant at which the shock wave reached the free surface of the sample was achieved by trial and error. Irradiation started several nanoseconds before the shock wave reached the surface, and the diffraction pattern of the structure of the compressed material was recorded through the layer of uncompressed material and the shock front. For this reason, the diffraction pattern consisted of two superposed patterns: 1) reflection from the initial structure of the sample and 2) reflection from the structure of the dynamically compressed material. Two peaks were recorded in the photographs obtained in Refs. 20 and 22. The first peak, having the larger diffraction angle, corresponds to an equilibrium state of the structure of the compressed material, and the second peak coincides with the peak of the initial structure of the sample. If it is assumed that the peak of the dynamical state of the structure is superposed on the peak of the initial state, it follows that the diffraction pattern recorded from the dynamically compressed lithium fluoride, presented in the present work, is identical to that of Refs. 20–22.

The formation of a nonequilibrium structural component can be understood if, by analogy with the results obtained for the silicon iron structure, the dynamical deformation of the lithium fluoride structure is interpreted assuming compression along the $\langle 111\rangle$ axis of the initial structure. In a deformation of this kind the lithium fluoride structure loses some symmetry elements of the initial packing and turns into a trigonal crystalline system. The unit cell of the Bravais lattice of the trigonal system—a rhombohedron—is determined by two parameters: the edge length l and the angle α between the edges. By varying the angle α of the rhombohedron it is possible to describe structural transformations accompanying deformation of the rhombohedron along its only axis [111] without leaving the trigonal system. The following particular cases are obtained in Ref. 18: 1) fcc structure, $\alpha = 60°$; 2) simple cubic structure with $\alpha = 90°$; 3) bcc structure with $\alpha = 109.46°$.

A characteristic feature of the deformation of the rhombohendron along the [111] axis is that the interplanar spacing $d_{(\bar{1}10)}$ (the Miller indices are written in a coordinate system whose basis vectors are determined by the edges of the rhombohedron) are preserved. The reason is that the deformation direction lies in the $(\bar{1}10)$ plane. This assertion is equally applicable to all planes of the zone whose axis is the [111] direction. Figure 4 shows the section by the plane $(\bar{2}20)$ [$(\bar{1}10)$ in the corrdinate system of the rhombohedron] of the cubic cell of the initial lattice of lithium fluoride and the direction [111] along which the structure is compressed. In order to specify the pattern, one of the four possible body diagonals of the cube was chosen and the $(\bar{2}20)$ plane is shaded. The interplanar spacing $d_{(\bar{2}20)}$ does not change under compression and tension along the [111] axis—the results of the experiment (Fig. 3a) where a $\langle 110\rangle$ lithium fluoride sample was investigated can be interpreted in this manner; the shock front in this sample was parallel to one of the $\{220\}$ planes according to the conditions of the measurements. Hence it follows that the deformation axis lies in the gas dynamic fracture plane.

For $\langle 100\rangle$ and $\langle 111\rangle$ samples the interpretation of the measurements is more complicated, since the compression of the initial structure along the [111] direction does not preserve the interplanar spaces $d_{(200)}$ and $d_{(111)}$—the body diagonals of the cubic cell do not lie in any plane of the form $\{200\}$ and $\{111\}$. Estimates show that for the $\langle 100\rangle$ sample (Fig. 3b) the recorded peak of the dynamical state of the structure, coinciding with the (200) peak of the initial structure [in the coordinate system of the rhombohedron—(110)], cannot be determined as the reflection from the (110) plane of the rhombohedron, since when the rhombohedron is compressed (its volume decreases), the spaceing $d_{(110)}$ can only decrease (see Fig. 11 below).

The indexing problem can be solved by taking into account the weak peak with the diffraction angle $\theta = 8.65°$, recorded in Fig. 3b. If the peak with $\theta = 10.16°$ is indexed as a reflection from the $(\bar{1}10)$ planes and the peak with $\theta = 8.65°$ is indexed as a reflection from the (100) planes of the rhombohedron, then the rhombohedron parameters are $\alpha = 103.6°$ and $l = 2.56$ Å and the ratio of the volume of the rhombohedron of the initial structure to the volume of the rhombohedron found is equal to the bulk compression of the sample. The diffraction data for the $\langle 100\rangle$ sample indicate that the initial structure is reoriented in the shock front to a

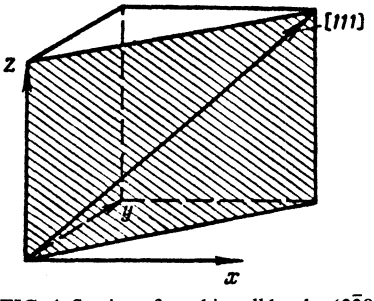

FIG. 4. Section of a cubic cell by the $(2\bar{2}0)$ plane.

position with respect to the plane of the front in which deformation conditions similar to those for the ⟨110⟩ sample are satisfied with the deformation remaining uniaxial. To underscore this fact, the microscopic process of deformation of a ⟨100⟩ sample can be conventionally divided into two stages: a) reorientation of the initial structure with preservation of cell volume and the condition $d_{(110)} = d_{(\bar{1}10)}$ with a possible change in the parameters of the rhombohedron: b) compression of the reoriented cell in the ⟨111⟩ direction with a reduction of its volume by a factor of σ. The appearance of a (100) reflection in the photograph can be explained by the fact that a small part of the layer of material studied is realized in an orientation when the (100) plane is in a reflecting position. The condition that the deformation axis be parallel to the gasdynamic fracture plane is not preserved for the structure of this part of the layer of the material.

The assumption that the initial structure is reoriented in the shock front is also used to explain the measurements of the parameters of the structure of the ⟨111⟩ sample. Only one reflection from the nonequilibrium structure is recorded in the photograph (Fig. 3b). This does not permit determining the parameters of the rhombohedron, but the reality of the existence of such a structural state is confirmed by an investigation of a ⟨111⟩ sample of potassium chloride under pressure above the phase transformation point $P = 2.1$ GPa.

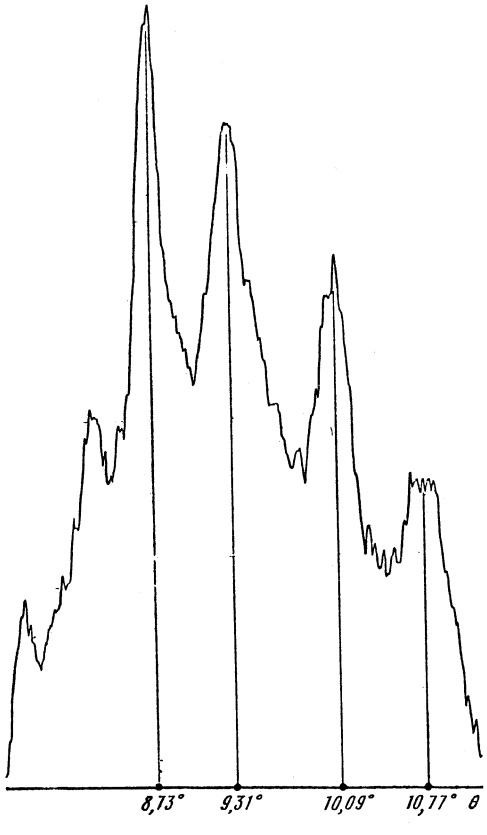

FIG. 5. Diffraction photograph of the structure of aluminum under pressure $P = 23$ GPa, $\sigma = 1.21$. The loading assembly is similar to that shown in Fig. 1. Peaks with $\theta \approx 9.31°$ and 10.77° were determined as reflections from (111) and (200) planes of the fcc lattice of the structure of the compressed material; peaks with $\theta \approx 8.73°$ and 10.09°, coinciding with the (111) and (200) peaks of the initial structure of the sample, are determined as reflections from ($\bar{1}10$) planes of two rhombohedral structures of the compressed material, which have rhombohedra with the same volumes but different angles α. Reflections formed by K_β Mo anode radiation can be seen on the left.

The Hugoniot-adiabat data for LiF and plexiglass were taken from Refs. 23 and 24.

3.4. Aluminum and potassium chloride

Fragments of the diffraction patterns of dynamically compressed aluminum and potassium chloride are displayed in Figs. 5 and 6. The photograph of the aluminum structure was obtained under a pressure $P = 23$ GPa and the photograph of potassium chloride was obtained under $P = 2$ GPa, below the phase transformation point. The data for the dynamical adiabat were taken from Ref. 14 in the case of aluminum and Ref. 25 in the case of potassium chloride. The diffraction patterns of the dynamical structures of both materials are qualitatively identical to the lithium fluoride patterns. Together with the analogous patterns of dynamical structures of crystals of materials with different packings (Be—hcp structure, Fe + 3% Si—bcc structure), they demonstrate the universal process of restructuring of the material under fast deformations, which results in the realization of two structural components—nonequilibrium and equilibrium—behind the shock front.

All existing experimental data indicate that the nonequilibrium component is formed as a result of the compression of the initial structures with fcc and bcc lattices along the crystallographic direction ⟨111⟩ and the compression of the hcp structure along [001], i.e., the C axis, the height of the hexagonal prism. The nonequilibrium component transforms on the shock front to an equilibrium state. Outside the front transformation process slows down, and this makes it possible to observe "frozen" structural states, in which part of the material has an equilibrium structure and part has a

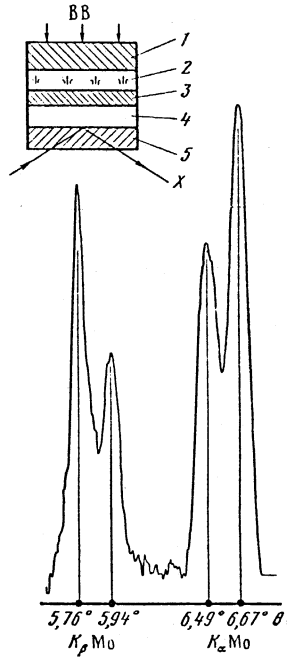

FIG. 6. Diffraction photograph of ⟨100⟩ structure of potassium chloride under pressure $P = 2$ GPa, $\sigma = 1.09$. Loading assembly: 1—striker (Cu, $L = 10$ mm, $W = 0.8$ km/sec); 2—polyethylene layer ($L = 6$ mm); 3—Cu layer ($L = 3$ mm); 4—sample ($L = 3$ mm); 5—Be layer ($L = 5$ mm). The chosen dynamical state was determined by the first shock wave, propagating along the sample, and appeared after the shock wave was reflected from the interface between the sample and the beryllium.

nonequilibrium structure. From this standpoint, the results of Refs. 6 and 11 can be interpreted as indicating realization of only a nonequilibrium component, which is in a "frozen" state different from uniaxial compressed state of the initial structure, in the investigated aluminum samples (alloy AD-1) behind the shock front.

3.5. Phase transition in potassium chloride

Single-crystal samples with ⟨100⟩ and ⟨111⟩ orientations were investigated in the pressure range 2.3–5.0 GPa.

The Hugoniot adiabat of potassium chloride in the region of the phase transformation was obtained in Refs. 25 and 26. A break was recorded in the adiabat at a pressure of $P = 2.1$ GPa. It was interpreted as a transition from a structure of the type NaCl to a structure of the type CsCl. This interpretation was confirmed experimentally under hydrostatic compression in a press.[27] Bridgman obtained the isothermal compression curve of potassium chloride up to pressure of 10 GPa.[28] Figure 7 displays Bridgman's results together with the data of Refs. 25 and 26. The dynamical adiabat contains a region where a transition occurs from one branch of the adiabat (initial branch) of the first phase to another branch—the adiabat of the second phase. This is the so-called metastable region of a mixture of phases, which extends from the onset of the transformation at $P = 2.1$ GPa up to $P = 3.1$ GPa according to Ref. 26 and $P = 5$ GPa according to Ref. 25. According to existing ideas, some of the material in the transitional region is in the first phase and some is in the second phase. The specific volumes of the material in different phases are determined by the dynamical adiabats of these phases, and the amount of each phase in the region of the mixture of phases can be determined by the lever rule.[25]

According to the data of Ref. 26, where a quartz pressure gauge with ≈ 1 nsec time resolution was employed, the potassium chloride samples with ⟨100⟩ and ⟨111⟩ orientations in the region of a mixture of phases are compressed up to metastable states of the Hugoniot-adiabat, common to samples of both orientations, but pressure reduction with a characteristic time ≈ 20 nsec was recorded for the ⟨111⟩ sample. This process was interpreted as decay of the first phase with complete transition of the material into an equilibrium state of the second phase. For the ⟨100⟩ sample the lifetime of the metastable state was longer than the time of the dynamical measurements (≈ 100 nsec) and no relaxation phenomena were observed.

The results of measurements of the structural parameters of potassium chloride reduce to the following.

1. For the ⟨100⟩ sample, compressed by a shock wave with amplitude $P = 2.9$ GPa (Fig. 8), a structural state with two components was recorded—equilibrium [(110) peak of a structure of the CsCl type with angle $\theta_{(110)} = 7.83°$] and nonequilibrum, referring to a rhombohedral trigonal system with angles $\theta_{(110)} = 7.04°$ and $\theta_{(\bar{1}10)} = 9.2°$. The primitive cells of the structural components have the same volume, equal to the volume of the primitive cell of the initial state of the structure decreased by a factor σ. The interplanar spacing $d_{(\bar{1}10)}$ of the nonequilibrium rhombohedron is equal to the interplanar spacing $d_{(220)}$ of the initial structure, i.e., the rhombohedron realized is idential to the rhombohedron of the initial structure compressed in the ⟨111⟩ direction by a factor of σ—a situation analogous to the one observed previously for structures of materials which do not undergo phase transformations on the Hugoniot adiabat in the pressure range investigated, the only difference being that the type of the equilibrium structure changed.

2. For the ⟨111⟩ sample, compressed by a shock wave with amplitude $P = 5$ GPa, a structural state with a nonequilibrium rhombohedral component and an equilibrium component of the CsCl type was also recorded. The parameters

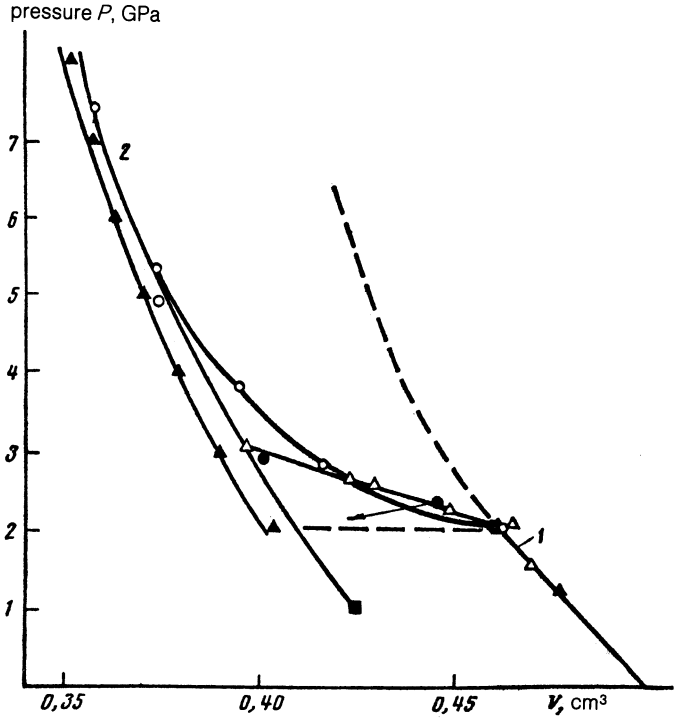

FIG. 7. Dynamical adiabat of potassium chloride: dots—experiment (▲—Ref. 28, ○—Ref. 25, △—Ref. 20, ●—x-ray diffraction measurements of this work, ■—boundary of existence of the second phase[25]), *1* and *2*—adiabats of the first and second phases, respectively. The arrow indicates the change in the specific volume of the ⟨111⟩ sample (according to Ref. 26).

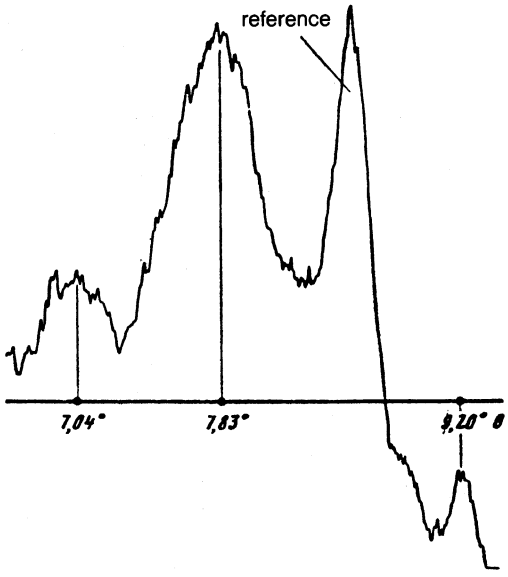

FIG. 8. Diffraction photograph of ⟨100⟩ potassium chloride structure under pressure $P = 2.9$ GPa, $\sigma = 1.23$. The loading assembly is similar to that shown in Fig. 1, but $W = 0.88$ km/sec. The peak with $\theta = 7.83°$ was determined as a reflection from the (110) plane of structure of the CsCl type with parameter $a = 3.687$ Å; the two other peaks with $\theta = 7.04°$ and 9.2° were determined as reflections from (110) and ($\bar{1}$10) planes of a rhombohedron with parameters $\alpha = 69.7°$ and $l = 3.885$ Å.

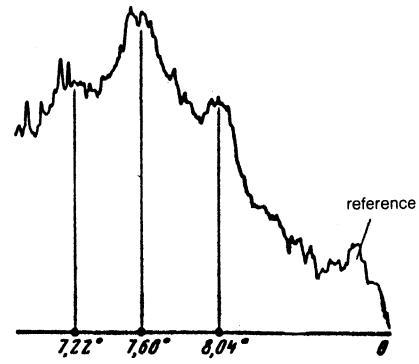

FIG. 9. Diffraction photograph of ⟨100⟩ potassium chloride structure under pressure $P = 2.3$ GPa, $\sigma = 1.13$. The loading assembly is similar to that shown in Fig. 1 but the striker (1) is different: Cu, $L = 10$ mm, $W = 0.62$ km/sec. A state on the metastable section of the adiabat was recorded. The peak with $\theta = 7.6°$ was determined as a reflection from the (110) plane of a structure of the CsCl type with parameter $a = 3.796$ Å, which is a nonequilibrium parameter at this pressure; the two other peaks with $\theta = 7.22°$ and 8.04° were determined as reflections from ($\bar{1}$10) and (110) planes of rhombohedron with parameters $\alpha = 95.5°$ and $l = 3.817$ Å.

of the structures realized correspond to compression of the material identical to the compression determined by the Hugoniot-adiabat.

3. For the ⟨100⟩ sample, compressed by a shock wave with amplitude $P = 2.3$ GPa (Fig. 9), two nonequilibrium structures were recorded. One structure belongs to a rhombohedral system and the other, with rhombohedron angle $\alpha = 90°$, is identical to a structure of the CsCl type. The parameters of the structures correspond to the density of the material on the metastable section of the adiabat.

4. For the ⟨111⟩ sample, compressed by a shock wave with amplitude $P = 2.3$ GPa (Fig. 10), a diffraction pattern interpreted as a superposition of several diffraction patterns on one another was recorded, i.e., it was assumed that a nonuniform structural state, when the layer of matter under study decomposes into a series of macroscopic regions with different rhombohedral structures, was realized.

We present below the results of a calculation, based on the data of Fig. 10, of the parameters of the structures which were realized. The following approach was used to calculate the parameters of the rhombohedron: The experimentally measured quantities are the interplanar spacing d and the specific volume V of the sample. Figure 11 shows the distances $d_{(110)}$, $d_{(\bar{1}10)}$, $d_{(111)}$, and $d_{(100)}$ as a function of the angle α of the rhombohedron, where the ratio of the volume of the rhombohedron to the cube of the interplanar spacing $-(M/A)\,V/d^3$, where M is the molar mass of the material and A is Avogadro's number—is plotted along the ordinate

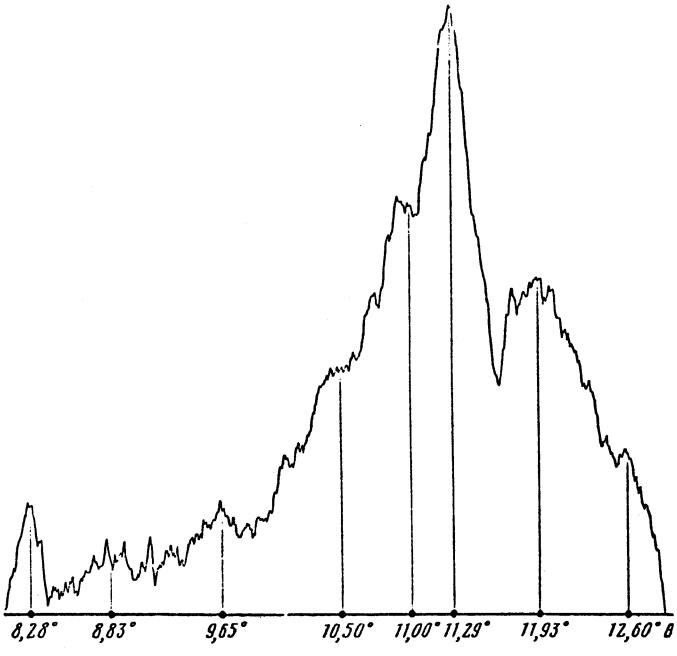

FIG. 10. Diffraction photograph of ⟨111⟩ potassium chloride structure under pressure $P = 2.3$ GPa, $\sigma = 1.13$. The loading assembly is the same as in Fig. 9.

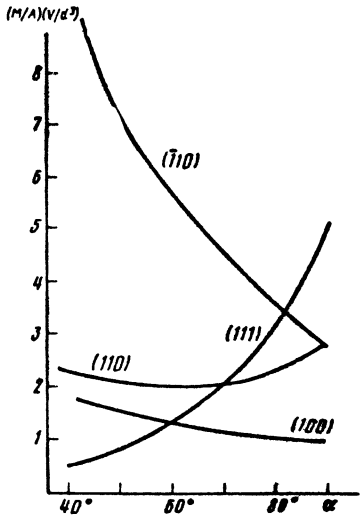

FIG. 11. Interplanar spacings as a function of the rhombohedron angle α. M—molar mass of the investigated material; A—Avogadro's number; V—specific volume of the material.

axis. The ratio V/d^3 determines the angle α and then l—the parameters of the rhombohedron, knowing which makes it possible to calculate the diffraction pattern and compare it with the photograph. In the calculation the specific volume of the material was taken to be $V = 0.425$ cm^3/g, which is different from the value $V_H = 0.442$ cm^3/g found from the Hugoniot-adiabat at $P = 2.3$ GPa. The choice was determined by the agreement between the computation results and the data in the photograph and was substantiated by the existence of relaxation of the density of the material for the ⟨111⟩ sample, as observed in Ref. 26. The results of the calculations are summarized in Table I, where the parameters of the realized rhombohedra, arranged sequentially by increasing angle α, are presented in the second and third columns. The diffraction angles and the reflection indices are presented in the fourth, fifth, and sixth columns.

The interpretation of the computational results is based on the following assumptions: a) reorientation of the initial structure and uniaxial compression along the ⟨111⟩ axis of the structure occurred in the shock front: b) transformation of the nonequilibrium structure into an equilibrium structure occurred within the shock front through intermediate states, which can be arranged in a sequence approaching the equilibrium state. The difference between the angles of the equilibrium and nonequilibrium rhombohedra can be used as the parameter characterizing the degree of departure from equilibrium. The transformation occurred at a constant density of the material, and the transformation rate was not the same everywhere in the layer of material studied. After the shock front has passed, the structural state becomes "frozen," and the transformation rate decreases. According to the data in Fig. 10, the most pronounced peaks refer to structures with the rhombohedron angles given in Table I. If the last rhombohedron with $\alpha = 90°$ is an equilibrium structure and the first rhombohedron with $\alpha = 41.8°$, "genetically" related with the orientation of the ⟨111⟩ sample with respect to the shock front, is oriented predominately so that its $(\bar{1}10)$ plane is turned toward the shock front, then the two others, according to the data in Fig. 11, have additional symmetry elements which increase the repetition factor for reflections with diffraction angles $\theta = 11.93°$ and $8.28°$. The difference between the rhombohedron angles for the intermediate structure No. 2 (Table I) and for the state with $d_{(\bar{1}10)} = d_{(111)}$ (Fig. 11) falls within the limits of the error of measurement. The computational results demonstrate a characteristic feature of structural transformations accompanying a transition from a uniaxially compressed initial structure to an equilibrium structure—the rhombohedron evolves through the variation of its angle over a definite range: from 41.8 to 90° under the conditions of the experiments under discussion here.

3.6. Potassium choloride under short-time ($3\cdot10^{-7}$ sec) dynamical loading

The nonequilibrium character of the processes accompanying rapid deformation of a material under short-time ($\sim 10^{-7}$ sec) dynamical loads was noted in Ref. 29. Photographs of the structure of a ⟨100⟩ sample of potassium chloride under pressure $P = 1.5$ GPa were made in order to obtain information about the structures which are realized under such loading conditions. Pressure was generated in the sample by a thin (1 mm) dielectric striker, accelerated up to $W = 0.8$ km/sec by an electric explosion of a foil. The technology of the acceleration assembly and the recording scheme are described in Ref. 9.

The characteristic difference between the photographs made under conditions of reduced loading time ($\approx 3\cdot10^{-7}$ sec) from the series of experiments (see Fig. 6) in which the loading time is of the order of several microseconds is that there is no equilibrium structural component. This distinction is associated with the nonequilibrium small thickness of the shock front. Under such loading conditions, there is not enough time for the comparatively slow transformation of a

TABLE I. Results of calculations of the parameters of the structure of ⟨111⟩ potassium chloride under presssure $P = 2.3$ GPa.

Structural state	Rhombohedron parameters		$\theta_{(222)}$	$\theta_{(\bar{1}10)}$	$\theta_{(200)}$
	α	l, Å			
Reoriented and uniaxially compressed initial structure of the sample	41,8°	5,076	8,83°	11,29°	13,40°
Intermediate structure No. 1	60,0°	4,200	11,93°	9,71°	11,93°
Intermediate structure No. 2	81,2°	3,790	16,5°	8,28°	11,00°
Equilibrium structure of the type CsCl	90,0°	3,750	19,15°	7,69°	10,91°

uniaxially deformed initial structure to "acquire" sufficient material with equilibrium structure for recording. According to estimates[29] of the equilibrium thickness of shock fronts for aluminum, at pressure $P = 10$ GPa the thickness reaches several microns and the residence time of the material in the viscous shock zone is ~ 1 nsec. This estimate can serve as a scale of the space-time dimensions of the rapid restructuring of shock-compressed cyrstals of materials not undergoing phase transformations in the investigated range of dynamical pressures.

For crystals of materials which do undergo phase transformations on the Hugoniot adiabat, significantly larger space-time scales of restructuring are characteristic. Under these conditions, the restructuring of the chemical bond, dictating the rate of structural transformations, is evdiently determining. Thus, according to estimates made in Ref. 25, at pressure $P = 2.3$ GPa the thickness of the front of the wave of phase transformation, traversing a distance ~ 10 mm along a ⟨100⟩ sample of potassium chloride, is ~ 500 μm, which is at least two orders of magnitude greater than the estimates of the thickness of a viscous shock for crystals in which phase transformations do not occur. For shock-front thicknesses such that the residence time of the material in the viscous shock is appreciably shorter than the restructing time of the chemical bond, structural states similar to those presented in Fig. 10 can apparently remain behind the shock front.

In conclusion we note that the recorded diffraction patterns cannot be understood on the basis of existing ideas physical processes occurring with rapid deformations of a material. The concepts of dislocation kinetics,[30,31] which are the basis for these ideas, do not incorporate the uniaxial structural compression process which changes the packing symmetry of the atoms. Apparently, the representations of restructing of chemical bonds in the condensed state of the material under dynamical loads with extremely high deformations rates $> 10^4$ sec^{-1} must be modified.

4. CONCLUSIONS

1. The initial structure of beryllium crystal compresses along the C axis—the height of the hexagonal prism—without any indications of any relaxational processes.

2. For cubic crystals a structural state containing equilibrium and nonequilibrium components was recorded. The nonequilibrium component belongs to the rhombohedral system.

3. Departure from equilibrium arises in the shock front as a result of uniaxial compression of the initial structure along one of the body diagonals of its cubic cell, which then transforms into an equilibrium state.

4. The parameters of the realized structural components correspond to compression of the material on the Hugoniot-adiabat.

5. For potassium chloride under pressures below and above the phase transformation point, structural states containing equilibrium and nonequilibrium components are realized. An equilibrium component of the NaCl type is realized below the phase transformation point and a component of the CsCl type is realized above the phase transformation point. The nonequilibrium components belong to the rhombohedral system in the entire range of pressures studied.

[1]L. A. Egorov, A. A. Lukashev, E. V. Nitochkina, and Yu. K. Orekin, Prib. Tekh. Eksp., No. 2, 200 (1968).
[2]L. A. Egorov, E. V. Nitochkina, and Yu. K. Orekin, Pis'ma Zh. Eksp. Teor. Fiz. **16**, 8 (1972) [JETP Lett. **16**, 4 (1972)].
[3]A. C. Mitchell, Q. Johnson, and L. Evans, Rev. Sci. Instrum. **44**, 597 (1973).
[4]E. Jamet and F. Bauer, *Comportement des Denses sous Hautes Pressions*, Dinamique, Paris (1978), p. 409.
[5]F. Muller and E. Schulte, Z. Naturforsch. A **33**, 918 (1978).
[6]L. V. Al'tshuler, L. A. Egorov, E. V. Nitochkina, and Yu. K. Orekin, Zh. Eksp. Teor. Fiz. **81**, 672 (1981) [Sov. Phys. JETP **54**(2), 359 (1981)].
[7]Q. Johnson, A. C. Mitchell, and I. D. Smith, Rev. Sci. Instrum. **51**, 741 (1980).
[8]N. I. Zavada, M. A. Manakova, and V. A. Tsukerman, Prib. Tekh. Eksp., No. **2**, 164 (1966).
[9]A. I. Barenboim, L. A. Egorov, and V. G. Kalinin, Prob. Tekh. Eksp., No. 1, 189 (1992).
[10]F. Jamet and G. Thomer, Proceedings of the International Congress on High Speed Photography, Nice (1972), p. 291.
[11]E. B. Zaretskiĭ, G. I. Kanel', P. A. Mogilevskiĭ, and V. E. Fortov, Teplofiz, Vys. Temp. **29**, 1002 (1991).
[12]L. V. Al'tshuler, Usp. Fiz. Nauk **85**, 197 (1965) [Sov. Phys. Usp. **8**(1), 52 (1965)].
[13]H. Lipson and H. Steeple, *Interpretation of X-Ray Powder Diffraction Patterns*, St. Martin's Press, N.Y., 1970 [Russian translation, Mir, Moscow, 1972, p. 179].
[14]L. V. Al'tshuler, A. A. Bakanova, I. P. Dudoladov *et al.*, Zh. Prikl. Mekh. Tekh. Fiz., No. 2, 3 (1981).
[15]L. I. Mirkin, *Handbook of X-Ray Structural Analysis of Polycrystals* [in Russian], Fizmatgiz, Moscow, 1961, p. 97.
[16]M. Podcarova, K. Godwod, J. Bak-Misiok *et al.*, Phys. Status Solidi A **106**, 17 (1988).
[17]E. C. Zukas, C. H. Fowler, F. S. Minshall, and J. O'Rourke, Trans. Metallurg. Soc. AIME **227**, 746 (1963).
[18]A. Kelly and G. Groves, *Crystallography and Crystal Defects*, Addison Wesley, Reading, MA, 1970 [Russian translation, Mir, Moscow, 1974, pp. 38–53].
[19]A. M. Podurets, A. I. Barenboim, V. V. Pul', and R. F. Trunin, Fiz. Zemli, No. 6, 26 (1989).
[20]Q. Johnson, A. C. Mitchell, and L. Evans, J. Appl. Phys. Lett. **21**, 29 (1972).
[21]Q. Johnson and A. C. Mitchell, High-Press. Sci. and Technology, Proceedings of the 5th AIRAPT Conference, Le Creusot, Pergamon Press, New York, 1978, p. 977.
[22]K. Kondo, A. Sawaoka, and S. Saito, High-Press. Sci. and Technology, Proceedings of the 6th AIRAPT Conference, Le Creusot, Plenum Press, New York, 1979, Vol. 2, p. 905.
[23]W. J. Carter, J. High Temp.-High Press. **5**, 313 (1973).
[24]M. van Thiel [Ed.], *Compendium of Shock Wave Data*, Lawrence Livermore Laboratory, Livermore, 1977.
[25]L. V. Al'tshuler, M. N. Pavlovskiĭ, and V. P. Drakin, Zh. Eksp. Teor. Fiz. **52**, 400 (1967) [Sov. Phys. JETP **25**(2), 260 (1967)].
[26]D. B. Hayes, J. Appl. Phys. **45**, 1208 (1974).
[27]J. D. Barnett and H. T. Hall, Rev. Sci. Instrum. **35**, No. 2 (1964).
[28]P. W. Bridgman, Proc. Am. Acad. Arts Sci. **76**, No. 1 (1945).
[29]B. F. Vorob'ev, U. Daubaev, I. P. Makarevich *et al.*, *Dynamical Processes in Gases and Solids* [in Russian], Leningrad University Press, Leningrad, 1984, p. 144.
[30]J. W. Taylor, J. Appl. Phys. **36**, 3146 (1965).
[31]J. R. Asay, D. L. Hicks, and D. B. Holdridge, J. Appl. Phys. **46**, 4316 (1975).

Translated by M. E. Alferieff